Journal of Materials Science: Materials in Electronics
https://doi.org/10.1007/s10854-018-9311-x

Adjustable microwave dielectric properties of $ZnO–TiO_2–ZrO_2–Nb_2O_5$ composite ceramics via controlling the raw ZrO_2 content and sintering temperature

Wendong Sun[1] · Huanfu Zhou[1] · Xianghu Tan[1] · Kangguo Wang[1] · Hong Ruan[1] · Hailin Zhang[1] · Xiaobin Liu[1,2] · Xiuli Chen[1]

Received: 1 April 2018 / Accepted: 17 May 2018

Abstract
A series of $2.5ZnO–(5-x)TiO_2–xZrO_2–2.5Nb_2O_5$ (abbreviated as ZTZN, $0.2 \le x \le 0.4$) composite ceramics were prepared by a solid state reaction method. The phase composition and microwave dielectric properties of the ceramics were investigated. X-ray diffraction patterns displayed the coexistence of $ZnTiNb_2O_8$ and $Zn_{0.17}Nb_{0.33}Ti_{0.5}O_2$ phases. With increasing the sintering temperature, the bulk density (ρ), permittivity (ε_r) and temperature coefficient of resonator frequency (τ_f) increased. With increasing the ZrO_2 content, the ρ firstly increased and then decreased, $Q \times f$ value increased, ε_r and τ_f value decreased. Importantly, the τ_f value of ZTZN ceramics ($0.2 \le x \le 0.4$) could be adjusted to near-zero. The $2.5ZnO–4.7TiO_2–0.3ZrO_2–2.5Nb_2O_5$ ceramics sintered at 1075 °C exhibited the best comprehensive performances of $Q \times f = 30{,}155$ GHz, $\varepsilon_r = 44$ and $\tau_f = 0.89$ ppm/°C, indicating that they are candidates for microwave devices.

1 Introduction

Recently, with the rapid development of modern wireless communication systems, the demands for high-performance microwave dielectric materials have increased considerably [1–3]. To meet these requirements, some critical characteristics, including lower sintering temperature [4], moderate permittivity (ε_r), high quality factor ($Q \times f$) and near-zero temperature coefficient of resonator frequency (τ_f), should be considered mainly. Furthermore, high relative permittivity (ε_r) achieves the miniaturization of components because the size of the resonator is inversely related to $\sqrt{\varepsilon_r}$. Low dielectric loss (tan δ) or more conveniently high Q value (1/tan δ) maximizes the signal discrimination [5]. High temperature-stability demands that the τ_f should be less than 5 ppm/°C and ideally be as near-zero [6]. Many ceramics exhibited excellent microwave dielectric properties, such as $Mg/CoCu_2Nb_2O_8$ [7], $ZnMnW_2O_8$ [8], $Zn(Li_{2/3}Ti_{4/3})O_4$ [9] and Li_2WO_4 [10], but the large positive or negative τ_f values limited their further industrial applications. Generally, two methods are used to adjust the τ_f values of microwave dielectric materials. One is mixing component materials with opposite τ_f values [3, 11], such as $(1-x)ZnAl_2O_4–xTiO_2$, $(1-x)ZnAl_2O_4–xCaTiO_3$ [12]. The other is forming solid solutions, such as $(Li_{0.5}Bi_{0.5})_xBi_{1-x}Mo_xV_{1-x}O_4$ [13], $Ba_{3.75}Nd_{9.5}Ti_{18-z}(Mg_{1/3}Nb_{2/3})_zO_{54}$ [14]. Remarkably, the former method was limited because the microwave dielectric properties would be degraded seriously.

Kim et al. [15] reported that the $2.5ZnO–2.5Nb_2O_5–5TiO_2$ (ZNT) ceramic sintered at 1100 °C showed excellent microwave dielectric properties with $\varepsilon_r = 58$, $Q \times f = 16{,}300$ GHz and $\tau_f = -10$ ppm/°C. In addition, Kim et al. [16] reported that the addition of ZrO_2 could be used to adjust the τ_f values of ceramics from the positive value to near-zero, such as $Zr_{1-x}(Zn_{1/3}Nb_{2/3})_xTiO_4$. Song et al. [17] reported that Ti^{4+} could be substituted by Zr^{4+} because the Ti^{4+} and Zr^{4+} have similar ionic radius [18]. In the present work, ZrO_2 was served to adjust the τ_f values by the substitution of Zr^{4+} for Ti^{4+}. Furthermore, the phase composition, microstructure

✉ Huanfu Zhou
zhouhuanfu@163.com

✉ Xiaobin Liu
xblgut@glut.edu.cn

[1] Collaborative Innovation Center for Exploration of Hidden Nonferrous Metal Deposits and Development of New Materials in Guangxi, Key Laboratory of New Processing Technology for Nonferrous Metals and Materials, Ministry of Education, School of Materials Science and Engineering, Guilin University of Technology, Guilin 541004, China

[2] College of Information Science and Engineering, Guilin University of Technology, Guilin 541004, China

Published online: 22 May 2018

and microwave dielectric properties of $2.5ZnO–(5-x)TiO_2–xZrO_2–2.5Nb_2O_5$ ceramics were also investigated.

2 Experimental procedure

High-purity raw materials (≥ 99%, Sinopharm Chemical Reagent Co., Ltd., Shanghai, China) of ZnO, ZrO_2, TiO_2 and Nb_2O_5 were used to prepare the ceramics samples by a common solid state reaction method. According to the stoichiometry of $ZnO:TiO_2:ZrO_2:Nb_2O_5 = 2.5:(5-x):x:2.5$ ($x = 0.2$, 0.3, 0.4), the raw powders were mixed in alcohol medium and milled with zirconia balls for 4 h. The mixtures were quickly dried and calcined at 900 °C for 4 h. Then the powders were milled via the same method as mentioned above for the second time. After stoving and sifting, the powders were mixed with 5 wt% polyvinyl alcohol (PVA) and uniaxially pressed into cylinders with 12 mm in diameter and 5 mm in thickness under the pressure of about 150 MPa. Finally, the samples were sintered over a temperature range of 975–1125 °C for 4 h in air at a heating rate of 5 °C/min.

The crystal structures of the specimens were identified by an X-ray diffraction (XRD) with CuK_α radiation generated at 40 kV and 40 mA (Model X'Pert PRO, PANalytical, Almelo, Holland). The surface morphology of ceramics was studied by a scanning electron microscopy (SEM) (Model JSM6380-LV SEM, JEOL, Tokyo, Japan). The bulk densities of the sintered ceramic were measured by the Archimedes method. Dielectric behaviors in microwave frequencies were measured by the $TE_{01\delta}$ shielded cavity method using a Network Analyzer Model E5071C, Agilent Co., CA, 300 kHz–20 GHz. The temperature coefficients of resonant frequency (τ_f) were measured by the open cavity method using an invar cavity in a temperature chamber (DELTA9039, Delta Design, USA). The τ_f values were calculated by the following formula:

$$\tau_f = \frac{f_T - f_0}{f_0(T - T_0)} \quad (1)$$

where f_T, f_0 are the $TE_{01\delta}$ resonant frequencies at temperature T (85 °C) and T_0 (25 °C), respectively.

3 Results and discussion

Figure 1 demonstrates the XRD patterns of ZTZN ($x = 0.3$) ceramics sintered at different temperatures. The diffraction peaks of ceramics could be indexed according to the patterns of $ZnTiNb_2O_8$ (PDF:00-048-0323, *Pbcn*, a = 4.6766 Å, b = 5.6656 Å, c = 5.0163 Å, $\alpha = \beta = \gamma = 90°$, V = 132.91 Å^3 and $Z = 1.00$) and $Zn_{0.17}Nb_{0.33}Ti_{0.5}O_2$ (PDF:00-039-0291, P42/*mnm*, a = 4.6739 Å, b = 4.6739 Å, c = 3.0214 Å,

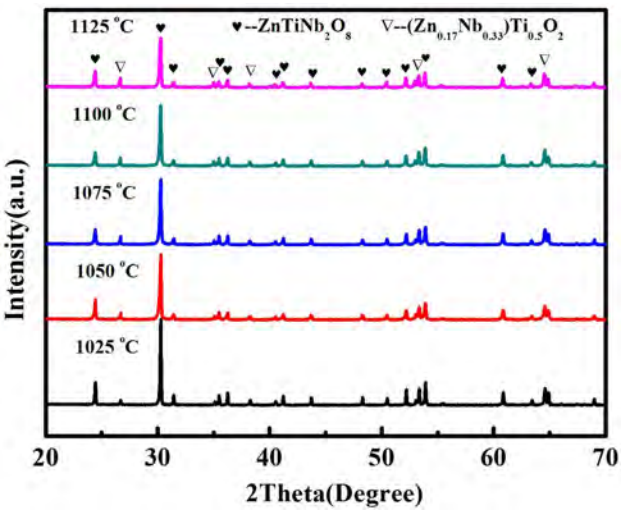

Fig. 1 XRD patterns of ZTZN ($x = 0.3$) ceramics sintered at different temperatures for 4 h

Table 1 The phase identification and their relative mass fraction of ZTZN ($x = 0.3$)

Condition	Phase	PDF code	wt (%)
ZTZN (1025 °C)	$ZnTiNb_2O_8$	00-048-0323	94.9
	$Zn_{0.17}Nb_{0.33}Ti_{0.5}O_2$	00-039-0291	5.1
ZTZN (1050 °C)	$ZnTiNb_2O_8$	00-048-0323	91.4
	$Zn_{0.17}Nb_{0.33}Ti_{0.5}O_2$	00-039-0291	8.6
ZTZN (1075 °C)	$ZnTiNb_2O_8$	00-048-0323	89.0
	$Zn_{0.17}Nb_{0.33}Ti_{0.5}O_2$	00-039-0291	11.0
ZTZN (1100 °C)	$ZnTiNb_2O_8$	00-048-0323	87.8
	$Zn_{0.17}Nb_{0.33}Ti_{0.5}O_2$	00-039-0291	12.2
ZTZN (1125 °C)	$ZnTiNb_2O_8$	00-048-0323	84.3
	$Zn_{0.17}Nb_{0.33}Ti_{0.5}O_2$	00-039-0291	15.7

$\alpha = \beta = \gamma = 90°$, V = 66.00 Å^3 and $Z = 2.00$) phases [19, 20]. The phase identification and their relative mass fractions are listed in Table 1. It can be seen that $ZnTiNb_2O_8$ phase gradually transformed into $Zn_{0.17}Nb_{0.33}Ti_{0.5}O_2$ phase with increasing the temperature from 1025 to 1125 °C. In addition, the lattice parameters of the two phases as a function of Zr content are listed in Table 2. Figure 2 shows the XRD patterns of the ZTZN ceramics sintered at 1025 °C for 4 h. The ZrO_2 phase was not observed in ceramics, because both Zr^{4+} and Ti^{4+} are tetravalent ions, and the ionic radius of Zr^{4+} (0.72 Å) is similar to that of Ti^{4+} (0.68 Å). Then Zr^{4+} equivalently substitutes Ti^{4+}, showing that Zn(Ti, Zr)Nb_2O_8 and $[Zn_{0.17}Nb_{0.33}(Ti, Zr)_{0.5}]O_2$ solid solution were formed [21]. With increasing the ZrO_2 content, the intensity of (111) diffraction peak enhanced gradually, and the diffraction intensity of (110) decreased gradually, which indicates that the addition of ZrO_2 hindered the process of

Table 2 The lattice parameters of the $ZnTiNb_2O_8$ and $Zn_{0.17}Nb_{0.33}Ti_{0.5}O_2$ phases as a function of the Zr content

Phase	Zr Content	a (Å)	b (Å)	c (Å)	α (°)	β (°)	γ (°)
$ZnTiNb_2O_8$	0 [19]	4.6766	5.6656	5.0163	90	90	90
	0.2	4.5262	5.6860	5.3037	90	90	90
	0.3	4.7335	5.6843	5.0360	90	90	90
	0.4	4.5345	5.6835	5.3075	90	90	90
$Zn_{0.17}Nb_{0.33}Ti_{0.5}O_2$	0 [20]	4.6739	4.6739	3.0214	90	90	90
	0.2	5.1619	5.1619	3.6260	90	90	90
	0.3	5.1633	5.1633	3.5836	90	90	90
	0.4	5.1658	5.1658	3.6270	90	90	90

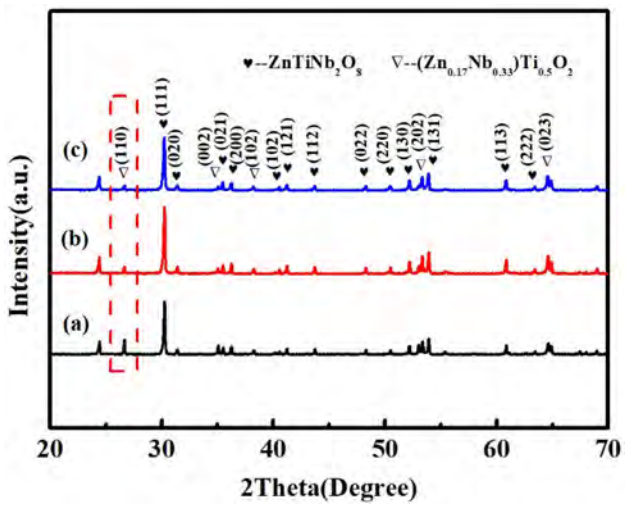

Fig. 2 XRD patterns of ZTZN ceramics sintered at 1025 °C for 4 h: (*a*) $x=0.2$, (*b*) $x=0.3$, (*c*) $x=0.4$

phase transformation. Further, the increase of ZrO_2 content improved the phase transformation temperature and hindered the phase transformation [20], which induces that $Zn_{0.17}Nb_{0.33}Ti_{0.5}O_2$ phase transformed into $ZnTiNb_2O_8$ phase.

Figure 3 illustrates the SEM images of ZTZN ceramic ($x=0.3$) sintered at different temperatures for 4 h. It can be seen that the grain size of ceramics increased with the increase of sintering temperature. Moreover, the microstructure of ceramic also became denser due to the decrease of pores. Energy dispersive spectrometer (EDS) analysis of the ZTZN ceramic ($x=0.3$) sintered at 1025 °C is listed in Table 3. With the help of EDS analysis, it could be confirmed that Zr has diffused into crystal structure. Figure 4 demonstrates the SEM images of ZTZN ceramics sintered at 1025 °C for 4 h. ZTZN ceramics have a relatively denser microstructure. With increasing the ZrO_2 content, the average grain size of ceramics increased gradually because the total binding force of dispersed phase particles is less than the driving force of the grain boundary. It is well known that the microstructure of samples would be influenced by the phase composition, as shown in Fig. 2. In addition, the change of phase composition could also induce the decrease of pores for ceramics. In other words, the microstructure of ceramic has become more compact as the x increased.

The bulk density of ZTZN ceramics sintered at different temperatures is shown in Fig. 5a. The bulk density of the samples increased with increasing the sintering temperature, illustrating that the microstructure has become more compact. In addition, the bulk densities decreased slightly with increasing the ZrO_2 content, which may be the fact that some part of Ti^{4+} position were replaced by larger radius Zr^{4+} and cause the increase of unit cell volume.

Figure 5b shows the $Q\times f$ values of ZTZN ceramics sintered at different temperatures. It is well known that the $Q\times f$ values are influenced by phase composition, grain size, pores and etc. [22]. It was found that intrinsic loss and extrinsic loss were the main factors to affect the quality factor. Intrinsic loss is related to lattice vibration, and extrinsic loss consists of density, second phase, the surface structures and crystal defect [23, 24]. The microwave dielectric properties of pure $ZnTiNb_2O_8$ and $Zn_{0.17}Nb_{0.33}Ti_{0.5}O_2$ phases are listed in Table 4. The $Q\times f$ values of ZTZN ceramics increased firstly and decreased then with increasing the sintering temperature. Because $ZnTiNb_2O_8$ phase gradually transformed into $Zn_{0.17}Nb_{0.33}Ti_{0.5}O_2$ phase with increasing the sintering temperature. The maximum $Q\times f$ values for all compositions were obtained when the sintering temperature was 1025 °C. The grain size increased when the sintering temperature and the ZrO_2 content increased, which result in lower dielectric loss because a larger grain will lead to less grain boundary and lattice mismatch [25, 26]. With increasing x values, $Zn_{0.17}Nb_{0.33}Ti_{0.5}O_2$ phase with lower $Q\times f$ value ($Q\times f=15{,}000$ GHz) in ZTZN ceramics decreased and $ZnTiNb_2O_8$ phase with higher $Q\times f$ value ($Q\times f=52{,}900$ GHz) increased, leading to the increase of $Q\times f$ values for ZTZN ceramics with increasing x values. Moreover, when $x=0.3$, the ceramics sintered at 1000 °C exhibited good microwave dielectric properties of $Q\times f=31{,}904$ GHz, $\varepsilon_r=42$ and $\tau_f=-20.2$ ppm/°C.

The relative permittivity (ε_r) of ZTZN ceramics sintered at different temperatures is shown in Fig. 5c. The

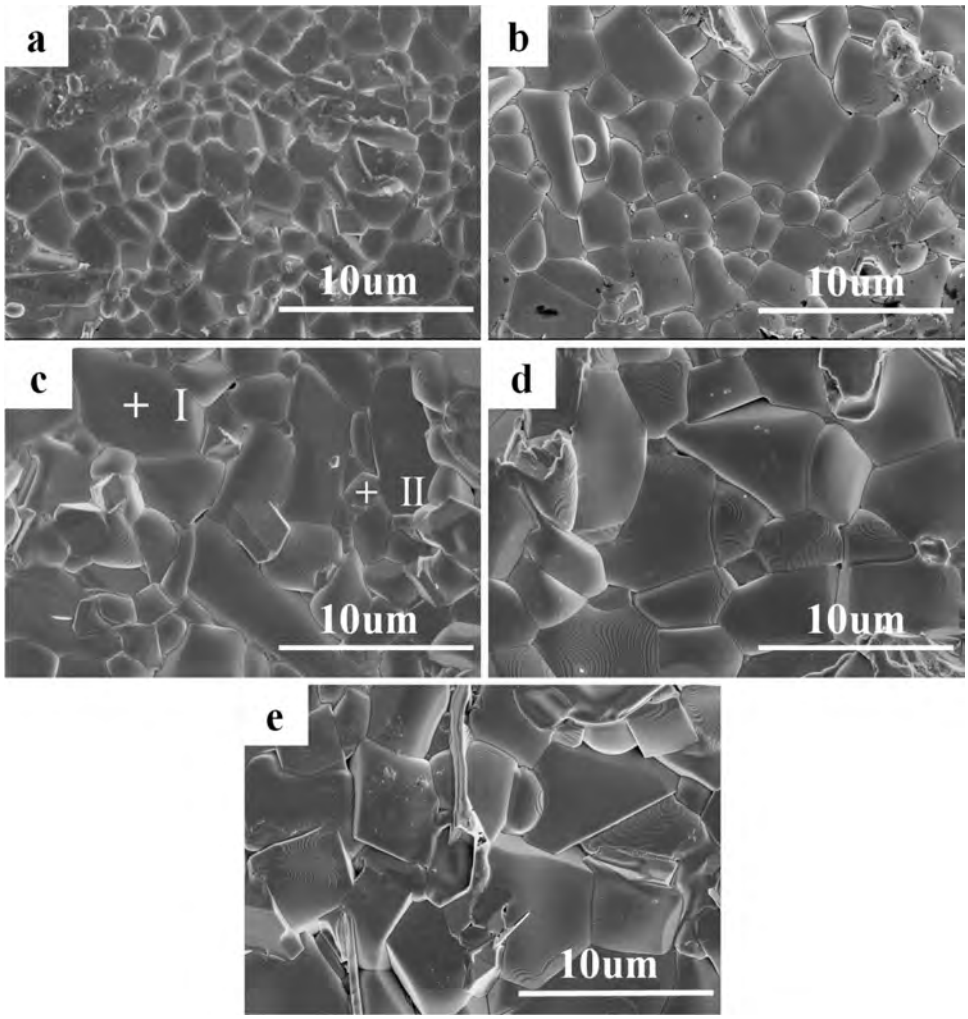

Fig. 3 SEM images of ZTZN ($x=0.3$) ceramics sintered at: **a** 1025 °C, **b** 1050 °C, **c** 1075 °C, **d** 1100 °C, **e** 1125 °C

Table 3 EDS analysis of ZTZN ceramics ($x=0.3$) sintered at 1025 °C

Region/ atomic (%)	Zn L	Ti K	Zr L	Nb L	O K
I	6.75	19.17	0.77	12.47	60.84
II	7.03	9.60	0.93	16.04	66.40

relationship between the ε_r and sintering temperature shows a similar trend to that of bulk density. With increasing the sintering temperature, $ZnTiNb_2O_8$ phase ($\varepsilon_r=34.3$) gradually transformed into $Zn_{0.17}Nb_{0.33}Ti_{0.5}O_2$ phase ($\varepsilon_r=94.5$). According to the logarithmic mixing law, the ε_r would change with the phase composition [27]. In other words, the phase composition and bulk density of the ceramic have great influence on the ε_r. As mentioned above, the addition of Zr induced the microstructure of ceramics more compact and hindered the formation of $Zn_{0.17}Nb_{0.33}Ti_{0.5}O_2$ phase, resulting in the decrease of ε_r for ZTZN ceramic. So the microstructure plays a significant role in determining the ε_r. When ZTZN ceramics were sintered at 1025 °C, $Zn_{0.17}Nb_{0.33}Ti_{0.5}O_2$ phase decreased with increasing x values from 0.2 to 0.4.

The temperature coefficient of resonator frequency (τ_f) for ZTZN ceramics system is shown in Fig. 5d. According to the previous reports, TiO_2 exhibited a positive τ_f value ($\tau_f=+450$ ppm/°C) [28]. So the τ_f values of ZTZN ceramics increased with increasing the TiO_2 content. However, the τ_f for all compositions could be adjusted to near-zero with controlling ZrO_2 content [29]. In addition, with increasing the sintering temperature, a part of $ZnTiNb_2O_8$ phase ($\tau_f=-56$ ppm/°C) transform into $Zn_{0.17}Nb_{0.33}Ti_{0.5}O_2$ phase ($\tau_f=+237$ ppm/°C). So the τ_f values of ZTZN ceramics also increased with increasing the temperature. Moreover, it has been mentioned above that the addition of ZrO_2 hindered the process of phase transformation and resulted in the decrease of $Zn_{0.17}Nb_{0.33}Ti_{0.5}O_2$ phase. Based the above reasons, the τ_f of the ZTZN ceramics system could also be adjusted to near zero. When the ZTZN ($x=0.2$) ceramics were sintered at 975 °C, the ceramics showed a near-zero τ_f value with 1.21 ppm/°C. When the ZTZN ($x=0.3$) ceramics

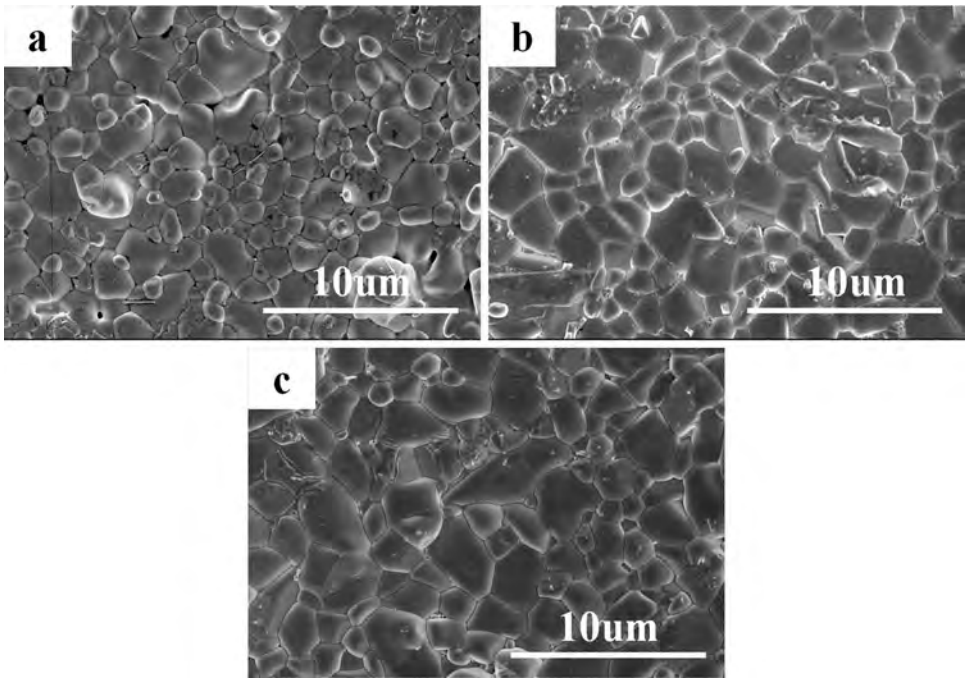

Fig. 4 SEM images of ZTZN ceramics sintered at 1025 °C for 4 h: **a** $x=0.2$, **b** $x=0.3$, **c** $x=0.4$

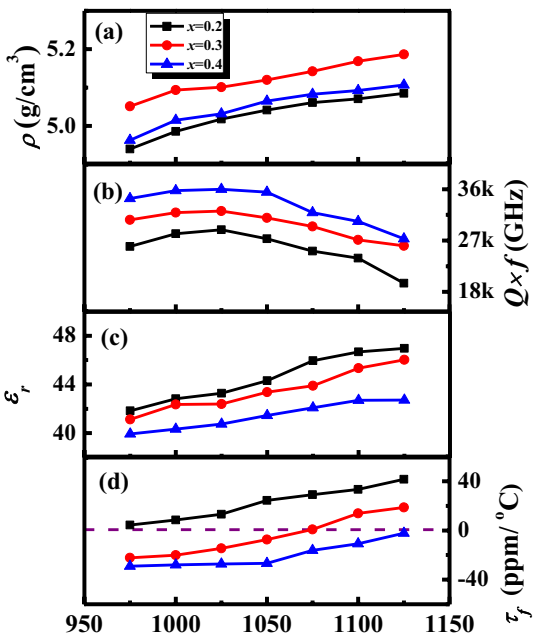

Fig. 5 Bulk density (ρ), permittivity (ε_r), $Q\times f$ and τ_f values of ZTZN ($x=0.2$, 0.3, 0.4) ceramics as a function of the sintering temperature

Table 4 Microwave dielectric properties of $ZnTiNb_2O_8$ and $Zn_{0.17}Nb_{0.33}Ti_{0.5}O_2$ phases

Phase	ε_r	$Q\times f$ (GHz)	τ_f (ppm/°C)	Refs.
$ZnTiNb_2O_8$	34.3	52,900	− 56.0	[28]
$Zn_{0.17}Nb_{0.33}Ti_{0.5}O_2$	94.5	15,000	+ 237.0	[28]

were sintered at 1075 °C, the ceramics exhibited a near-zero τ_f value with 0.89 ppm/°C. When the ZTZN ($x=0.4$) ceramics were sintered at 1125 °C, the ceramic showed a near-zero τ_f value with − 2.25 ppm/°C. It can be seen that the temperature of obtaining a near-zero τ_f value increased with increasing the ZrO_2 content.

4 Conclusion

With increasing the ZrO_2 content, the phase structure of ceramics partly transformed from $Zn_{0.17}Nb_{0.33}Ti_{0.5}O_2$ phase into $ZnTiNb_2O_8$ phase, causing the variation of the microwave dielectric properties. Besides, the sintering temperature also affects the microwave dielectric properties via changing phase composition. Generally, the τ_f for all compositions of ZTZN ceramics could be adjusted to near-zero by controlling the sintering temperature. Importantly, the $2.5ZnO–4.7TiO_2–0.3ZrO_2–2.5Nb_2O_5$ ceramics ($x=0.3$) sintered at 1075 °C exhibited the best comprehensive performances of $Q\times f=30{,}155$ GHz, $\varepsilon_r=44$ and $\tau_f=0.89$ ppm/°C, indicating that the ceramics system is a potential microwave dielectric material in commercial application.

Acknowledgements This work was supported by Natural Science Foundation of China (Nos. 11464009, 61761015 and 11664008), Natural Science Foundation of Guangxi (Nos. 2017GXNSFFA198011, 2015GXNSFDA139033 and 2017GXNSFDA198027) and Research Start-up Funds Doctor of Guilin University of Technology (No. GUTQDJJ2017133).

References

1. Z.Y. Zou, Z.H. Chen, X.K. Lan, W.Z. Lu, B. Ullah, X.H. Wang, W. Lei, Weak ferroelectricity and low-permittivity microwave dielectric properties of $Ba_2Zn_{(1+x)}Si_2O_{(7+x)}$ ceramics. J. Eur. Ceram. Soc. **37**, 3065–3071 (2017)
2. H.F. Zhou, J. Huang, X.H. Tan, Microwave dielectric properties of low-permittivity $CaMgSiO_4$ ceramic. J. Mater. Sci.: Mater. Electron. **28**, 15258–15262 (2017)
3. J. Guo, D. Zhou, H. Wang, Microwave dielectric properties of (1-*x*)$ZnMoO_4$-*x*TiO_2 composite ceramics. J. Alloys Compd. **509**, 5863–5865 (2011)
4. Z.G. Zang, X.S. Tang, Enhanced fluorescence imaging performance of hydrophobic colloidal ZnO nanoparticles by a facile method. J. Alloys Compd. **619**, 98–101 (2015)
5. C.L. Huang, M.H. Weng, Improved high *Q* value of $MgTiO_3$-$CaTiO_3$ microwave dielectric ceramics at low sintering temperature. Mater. Res. Bull. **36**, 2741–2750 (2001)
6. R. Freer, Microwave dielectric ceramics: an overview. Silic. Ind. **58**, 191–197 (1993)
7. R.C. Pullar, C. Lai, F. Azough, Novel microwave dielectric LTCCs based upon V_2O_5 doped $M^{2+}Cu_2Nb_2O_8$ compounds (M^{2+} = Zn, Co, Ni, Mg and Ca). J. Eur. Ceram. Soc. **26**, 1943–1946 (2006)
8. J.S. Kim, J.C. Lee, C.I. Cheon, H.J. Kang, Crystal structure and low temperature cofiring ceramic property of (1-*x*)(Li, Re)W_2O_8-*x*$BaWO_4$ ceramics (Re = Y, Yb). Jpn. J. Appl. Phys. **45**, 7397–7400 (2006)
9. H.F. Zhou, X.B. Liu, X.L. Chen et al., $ZnLi_{2/3}Ti_{4/3}O_4$: a new low loss spinel microwave dielectric ceramic. J. Eur. Ceram. Soc. **32**, 261–265 (2012)
10. D. Zhou, C.A. Randall, L.X. Pang, Microwave dielectric properties of Li_2WO_4 ceramic with ultra-low sintering temperature. J. Am. Ceram. Soc. **94**, 348–350 (2011)
11. K. Fukuda, R. Kitoh, I. Awai, Microwave characteristics of TiO_2BiO_3 dielectric resonator. Jpn. J. Appl. Phys. **32**, 4584–4588 (1993)
12. C.F. Tseng, P.S. Tsai, Microwave dielectric properties of (1-*x*) $ZnAl_2O_4$-*x*$CaTiO_3$ compound ceramic with controlled temperature coefficient. Ceram. Int. **39**, 75–79 (2013)
13. D. Zhou, W.G. Qu, C.A. Randall, Ferroelastic phase transition compositional dependence for solid-solution $[(Li_{0.5}Bi_{0.5})_xBi_{1-x}][Mo_xV_{1-x}]O_4$ scheelite-structured microwave dielectric ceramics. Acta. Mater. **59**, 1502–1509 (2011)
14. H.T. Chen, B. Tang, S. Duan et al., Microstructure and microwave dielectric properties of $Ba_{3.75}Nd_{9.5}Ti_{18-z}(Mg_{1/3}Nb_{2/3})_zO_{54}$ ceramics. J. Electron. Mater. **44**, 1081–1087 (2015)
15. D.H. Kim, C. An, Y.S. Lee et al., Microwave dielectric properties of ZnO-RO_2-TiO_2-Nb_2O_5 (R = Sn, Zr, Ce) ceramic system. J. Mater. Sci. Lett. **22**, 569–571 (2003)
16. K.S. Kim, S. Kim, H.K. Yun, O.Y. Soon, J.G. Park, Sintering behavior and microwave dielectric properties of the $Zr_{1-x}(Zn_{1/3}Nb_{2/3})_xTiO_4$ system with zinc-borosilicate glass. J. Ceram. Process. Res. **9**, 126–130 (2008)
17. F.S. Song, Y.M. Li, Z.X. Shen et al., Effect of TiO_2 addition amount on structure and microwave dielectric properties of $Zn_{0.8}Mg_{0.2}ZrNb_2O_8$ ceramic. J. Chin. Ceram. Soc. **43**, 1725–1730 (2015)
18. X.C. Liu, F. Gao, C.S. Tian, Synthesis, low-temperature sintering and the dielectric properties of the ZnO-(1-*x*)TiO_2-*x*SnO_2 (*x* = 0.04–0.2). Mater. Res. Bull. **43**, 693–699 (2008)
19. A. Baumgarte, R. Blachnik, New $M^{2+}M^{4+}Nb_2O_8$ phases. J. Alloys Compd. **215**, 117–120 (1994)
20. J. Andrade, M.E. Villafuerte-Castrejon, R. Valenzuela, A.R. West, Rutile solid solutions containing M^+(Li), M^{2+}(Zn, Mg), M^{3+}(Al) and M^{5+}(Nb, Ta, Sb) ions. J. Mater. Sci. Lett. **5**, 147–149 (1986)
21. S. Wu, J. Luo, Mg-substituted $ZnNb_2O_6$–TiO_2 composite ceramics for RF/microwaves ceramic capacitors. J. Alloys Compd. **509**, 8126–8129 (2011)
22. H.P. Wang, Q.L. Zhang, H. Yang, Low-temperature firing and microwave dielectric properties of ZnO–Nb_2O_5–TiO_2–SnO_2 ceramics with CuO–V_2O_5, Mater. Res. Bull. **40**, 1891–1898 (2005)
23. E.S. Kim, D.H. Kang, Relationships between crystal structure and microwave dielectric properties of $(Zn_{1/3}B_{2/3}{}^{5+})_xTi_{1-x}O_2$ (B^{5+} = Nb, Ta) ceramics. Ceram. Int. **34**, 883–888 (2008)
24. S.J. Penn, N.M. Alford, A. Templeton et al., Effect of porosity and grain size on the microwave dielectric properties of sintered alumina. J. Am. Ceram. Soc. **80**, 1885–1888 (1997)
25. L.X. Li, X. Ren, Q.W. Liao, Crystal structure and microwave dielectric properties of $Zn_{0.9}Ti_{0.8-x}Sn_xNb_{2.2}O_8$ ceramics. Ceram. Int. **38**, 3985–3989 (2012)
26. R.G. Hoagland, S.M. Valone, Emission of dislocations from grain boundaries by grain boundary dissociation. Philos. Mag. **95**, 112–131 (2015)
27. H.F. Zhou, X.H. Tan, J. Huang, Sintering behavior, phase structure and adjustable microwave dielectric properties of Li_2O-MgO-*n*TiO_2 ceramics ($1 \le n \le 5$). J. Mater. Sci.: Mater. Electron. **28**, 6475–6480 (2017)
28. P. Ruan, P. Liu, B.C. Guo, F. Li, Z.F. Fu, Microwave dielectric properties of ZnO-Nb_2O_5-*x*TiO_2 ceramics prepared by reaction-sintering process. J. Mater. Sci.: Mater. Electron. **27**, 4201–4205 (2016)
29. W. Lei, Z.Y. Zou, Z.H. Chen, B. Ullah, A. Zeb, Controllable τ_f value of barium silicate microwave dielectric ceramics with different Ba/Si ratios. J. Am. Ceram. Soc. **101**, 25–30 (2018)